Dalton Transactions

Accepted Manuscript

ROYAL SOCIETY OF CHEMISTRY

www.rsc.org/dalton

Crystal structures in $NaBa_{1-x}Ca_xPO_4$ system changed depending on the Ca substitution. Three kind of crystal structure were observed at x = 0, 1/3 and 0.5. New crystal structures were formed rather than formation of solid solutions between $NaBaPO_4$ and $NaCaPO_4$. Eu-doped samples exhibited emission maximum between 435 nm and 460 nm, depending on the amount of Ca.

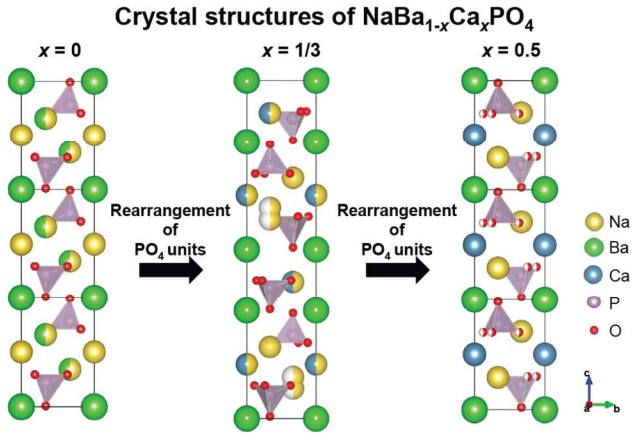

Journal Name

RSCPublishing

ARTICLE

Crystal Structures and Luminescence Properties of Eu^{2+}-activated new $NaBa_{0.5}Ca_{0.5}PO_4$ and $Na_3Ba_2Ca(PO_4)_3$

Cite this: DOI: 10.1039/x0xx00000x

Received 00th January 2012,
Accepted 00th January 2012

DOI: 10.1039/x0xx00000x

www.rsc.org/

Minsung Kim,[a] Makoto Kobayashi,[a] Hideki Kato,[a] Hisanori Yamane,[a] Yasushi Sato[b] and Masato Kakihana*[a]

$NaBa_{1-x}Ca_xPO_4:Eu^{2+}$ were synthesized by polymerizable complex method. New phases were observed at x = 1/3 and 0.5, which were identified by single-crystal XRD analysis as $Na_3Ba_2Ca(PO_4)_3$ and $NaBa_{0.5}Ca_{0.5}PO_4$ with trigonal system. Though both phases pretend to be the solid solutions between $NaBaPO_4$ and $NaCaPO_4$, they have different coordination environments and PO_4 orderings. 1 mol% Eu^{2+}-activated $NaBaPO_4$, $Na_3Ba_2Ca(PO_4)_3$, and $NaBa_{0.5}Ca_{0.5}PO_4$ exhibited emission maximum at 435 nm, 458 nm, and 460 nm, respectively. The shift of the emission maximum might be due to a change in the Eu-O bond length.

Introduction

Exploration of new compounds is required to meet demands from the modern society, because finding novel compounds often produce high-functional materials. At the same time, precise characterization of new compounds gives us novel knowledge of material chemistry, resulting in material design. For many years, a variety of approaches such as combinatorial method has been applied to finding new compounds. As a result, huge number of compounds has been found and their properties has been clarified. Nevertheless, new and useful compounds are reported in recent years[1]. The fact indicates that evolutional materials with high and unique functions are still hidden elsewhere.

Phosphates are widely recognized as important functional and structural materials and used in various fields. For example, tricalcium phosphate and hydroxyapatite are famous biomaterials because of their chemical similarity to natural bone, and good biocompatibility and bioactivity.[2] $LiFePO_4$ has excellent thermal stability, high cell voltage, and environmental benign property, therefore, it is applied in Li-batteries.[3] Also, rare-earth activated phosphate compounds are one of potential phosphors due to high brightness and stable physical and chemical properties.[4]

To date, we have succeeded in development of new thioaluminates through synthesis of solid solutions employing a reliable and compositionally-controllable synthesis method[5]. Studies on solid solution seem to be a effective way to find new compounds. Solid solutions of phosphate compounds have also been widely investigated, and several kinds of solid solution phosphates have been developed.[6] Examples of such solid solution phosphates include $NaSrPO_4$-$NaBaPO_4$, $KSrPO_4$-$NaSrPO_4$, and $KSrPO_4$-$(Ba,Sr)_2SiO_4$. Solid solutions of phosphate compounds with the formula $ABPO_4$, where A and B are mono- and divalent cations, respectively, have been investigated extensively. However, to the best of our knowledge, there are few reports on synthesis and properties of $NaBaPO_4$-$NaCaPO_4$ ($Na(Ba,Ca)PO_4$) solid solutions. One of the reasons may be due to differences between the crystal systems of $NaBaPO_4$ (trigonal) and $NaCaPO_4$ (orthorhombic) caused by large difference in ionic radius of Ba^{2+} and Ca^{2+}.

In this study, we have attempted the solution-based synthesis of $NaBaPO_4$-$NaCaPO_4$ solid solutions *via* polymerizable complex (PC) method using a water-soluble and stable P source developed by our group,[7] aiming at application for phosphor. Two novel compounds, $Na_3Ba_2Ca(PO_4)_3$ and $NaBa_{0.5}Ca_{0.5}PO_4$, were developed and their crystal structures were determined by single crystal X-ray analysis. In addition, photoluminescence properties of Eu^{2+}-doped samples were investigated.

Experimental Section

Synthesis of $NaBa_{1-x}Ca_xPO_4:Eu^{2+}$

Eu^{2+}-doped $NaBa_{1-x}Ca_xPO_4$ phosphors were synthesized *via* the PC method with polyethylene glycol-conjugated phosphate ester (PEG-P)[7] as a P source. PEG-P was synthesized from reactions among polyethylene glycol 300, phosphorus pentoxide, and polyphosphoric acid under a N_2 atmosphere at 353 K. Details of the PEG-P preparation procedure are described elsewhere.[7] Na_2CO_3 (99%, Kanto Chemical), $BaCO_3$ (99%, Kanto Chemical), $CaCO_3$ (99.99%, Kanto Chemical), and $Eu(NO_3)_3$ (prepared by the dissolution of Eu_2O_3 (99.9 %,

Furuuchi Chemical) in HNO_3) were dissolved in an aqueous solution of citric acid (CA) at a molar ratio of Na : Ba : Ca : Eu : P : CA = 1 : (1-x-y) : x : y : 1 : 12. In the present research, y was fixed to 0.01, that is, the 1 mol% Eu-doped samples were synthesized. To assist chelation, the mixture was heated at 353 K for 2 h, after which PEG-P and propylene glycol (PG) were added into the solution at a molar ratio of 1 : 8. The temperature was subsequently increased to 423 K to initiate gel formation by polyesterification.[8] After gel formation, the reaction mixture was heated at 1123 K in air to remove organic residues, and then reduced at 1273 K under a flow of Ar containing 4 % H_2 for 3 h. For crystal structure analysis, single crystals were prepared using the flux growth method. Samples without Eu dopant (x = 0.3 and 0.5) were mixed with NaCl as a flux at a weight ratio of 1:2 using an agate mortar and pestle. The mixture was formed into pellets, sealed under vacuum in a quartz ampoule, heated at 1273 K for 5 h, and then slowly cooled to 1073 K at a rate of 100 K h^{-1}. After subsequent cooling to room temperature, the single crystals were washed with distilled water. Colorless crystals with dimensions of 0.093 mm × 0.073 mm × 0.048 mm (x = 0.5) and 0.106 mm × 0.101 mm × 0.037 mm (x = 1/3) were used for single crystal X-ray diffraction (XRD) analysis.

Measurements and characterization

The crystal phases of the samples were identified by powder XRD (Bruker AXS; D2 Phaser) using a Cu Kα source (λ = 1.5418 Å) scanning 2θ from 10° to 70°. Rietveld analysis was conducted using the TOPAS software supplied by Bruker Co. Ltd. The emission and excitation spectra were collected at room temperature using a fluorescence spectrophotometer (Hitachi; F-4500) scanning the wavelength range of 200 nm to 600 nm. A quartz sample chamber was filled with phosphor powder and aligned within the fluorescence spectrometer to ensure that all the samples were subjected to measurements under the same conditions. Quantum efficiencies of the samples were evaluated with another fluorescence spectrometer (Jasco; FP-6500) equipped with a 150 W xenon lamp and an integrating sphere (Jasco; ISF-513). Emission lifetime (decay) was examined at room temperature by other fluorescence spectrometer (HORIBA; FluoroCube) employing a UV diode laser at 375 nm and their emission was monitored at 440 nm.

A single crystal was fixed to the tip of a glass fiber with epoxy resin and mounted to the goniometer of a single-crystal X-ray diffractometer (Rigaku; R-AXIS RAPID-II). X-ray diffraction data of the single crystals were collected using Mo Kα radiation with a graphite monochromator and an imaging plate. Unit cell refinement and absorption collection were performed with the programs RAPID-AUTO[9] and NUMABS,[10] respectively. The crystal structure was solved by direct methods using the SIR2004 program,[11] and structure parameters were refined by full-matrix least-squares on F^2 using the SHELXL-97 program.[12] All calculations were conducted on using the WinGX software package.[13] Crystal structure illustrations were prepared with the VESTA program.[14]

Result and discussion

Synthesis of $NaBa_{1-x}Ca_xPO_4$ solid solutions

Fig. 1 shows the XRD patterns of $NaBa_{1-x}Ca_xPO_4$:0.01Eu^{2+} with x = 0.0, 0.1, 0.2, 0.3, 0.4 and 0.5 reduced at 1273 K for 3 h in Ar/4 % H_2 atmosphere, and a simulated pattern of $NaBaPO_4$ from the Inorganic Crystal Structure Database (ICSD) #73704. The XRD pattern of the sample without Ca (x = 0) was in good agreement with that of trigonal (P-3m1) $NaBaPO_4$. The diffraction patterns of samples with x = 0.1 and 0.2 contained several additional peaks at 18.77°, 24.31°, 29.89°, and 32.80° as compared with $NaBaPO_4$. These additional peaks were not assigned to any known substances, but instead indicated the formation of a new crystal phase, denoted here as phase 1. The intensity of the peaks from phase 1 increased with increase of Ca substitution until x = 0.3, decreased at x = 0.4, and finally, the peaks disappeared at x = 0.5. Another unknown phase, denoted here as phase 2, was also observed. Phase 2 appeared from x = 0.3, and the corresponding peak intensity increased with increasing Ca content.

Crystal structures of new phases in $NaBa_{1-x}Ca_xPO_4$

The single crystal data are compared with that of $NaBaPO_4$ (ICSD #73704) in Table 1 (Crystallographic Information Frameworks (CIFs) of the crystals are provided as Supplementary Material). The single crystal analysis revealed that phase 1 was a trigonal system (P31c) with a composition of $Na_3Ba_2Ca(PO_4)_3$ (abbreviated as NBC321) and phase 2 was

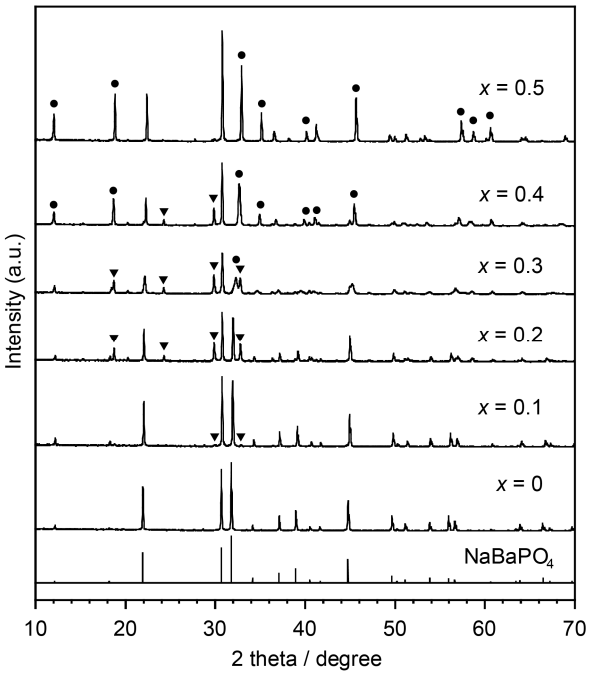

Fig. 1 XRD patterns of $NaBa_{1-x}Ca_xPO_4$:0.01Eu^{2+} solid solutions for x = 0 ~ 0.5 reduced at 1273 K for 3 h in Ar/4% H_2 atmosphere, and a simulated patterns of $NaBaPO_4$ (ICSD #73704); unknown phase 1 (▼) and phase 2 (●).

also a trigonal system (*P*-3*m*1, the same as $NaBaPO_4$) with a composition of $NaBa_{0.5}Ca_{0.5}PO_4$ (abbreviated as NBCP). The lattice constants of NBC321 were a = 5.4515(2) Å and c = 23.1283(8) Å, and those of NBCP were a = 5.4474(4) Å and c = 7.3624(5) Å. The cell volume (V) decreased from 198.37 $Å^3$ ($NaBaPO_4$) to 189.20(2) $Å^3$ (NBCP).

Table 1 Comparison of single crystal data of $Na_3Ba_2Ca(PO_4)_3$, $NaBa_{0.5}Ca_{0.5}PO_4$, and crystal data of $NaBaPO_4$ (ICSD #73704).

Formula		$NaBaPO_4$	$Na_3Ba_2Ca(PO_4)_3$	$NaBa_{0.5}Ca_{0.5}PO_4$
Abbr.		-	NBC321	NBCP
Crystal system		Trigonal	Trigonal	Trigonal
Space group		*P*-3*m*1	*P*31*c*	*P*-3*m*1
Lattice parameters	*a* (Å)	5.617(1)	5.4515(2)	5.4474(4)
	c (Å)	7.260(1)	23.1283(8)	7.3624(5)
	V($Å^3$)	198.37	595.24(6)	189.20(2)
Z		2	2	2
R indices (all data)		R = 0.057	R_1 = 0.0388 wR_2 = 0.0744	R_1 = 0.0168 wR_2 = 0.0408

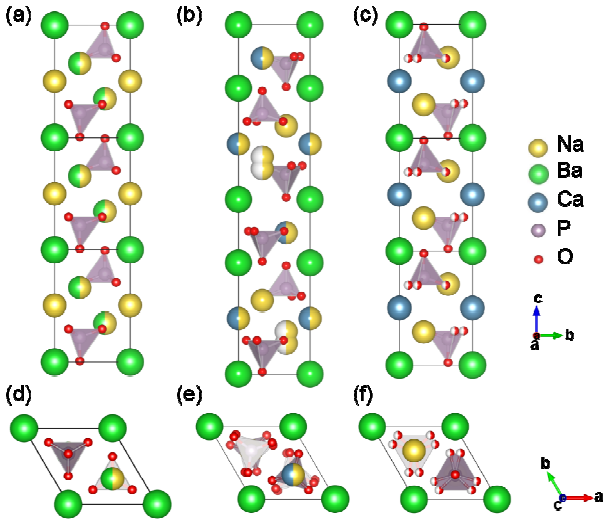

Fig. 2 Crystal structures of the (a,d) $NaBaPO_4$, (b,e) $Na_3Ba_2Ca(PO_4)_3$ and (c,f) NBCP visualized using VESTA crystal drawing software.[14]

Fig. 2 shows the crystal structures of (a) $NaBaPO_4$, (b) NBC321, and (c) NBCP. Atomic arrangements in the three crystals are similar. Both $NaBaPO_4$ and NBCP are isotropic structures of glaserite and were determined to have the same space group. However, the coordination numbers (CN) for each cation in $NaBaPO_4$ and NBCP were different. $NaBaPO_4$ and NBCP have three metal cation sites with coordination numbers 6, 10, and 12. In $NaBaPO_4$, Na^+ and Ba^{2+} exist at the CN 10 site with half occupancy. The remaining Na^+ and Ba^{2+} occupy the CN 6 and 12 sites, respectively. In NBCP, Ca^{2+}, Na^+, and Ba^{2+} occupy the CN sites 6, 10 and 12, respectively. The two compounds have the same crystal structure but different their coordination environments, therefore, NBCP is a new phase. The *c* axis of NBC321 is approximately three times larger than those of $NaBaPO_4$ and NBCP. In NBC321, PO_4 units are tilted with respect to the *c* axis, while those in $NaBaPO_4$ and NBCP are aligned with the axis. In addition, regularity of PO_4 unit direction in the NBC321 is different from others, though a series of $NaBa_{1-x}Ca_xPO_4$ pretend to be the solid solutions. In $NaBaPO_4$ and NBCP, Ba and Na/Ca alternate along the *c* axis, whereas in NBC321, a set of two Ba and Ca/Na propagates along the *c* axis. In a series of $NaBa_{1-x}Ca_xPO_4$, one of faces at PO_4 units faces to *ab* plane constructing by Na/Ca sites. In other words, the *ab* plane exists in between PO_4 faces. The ionic radius of Ba^{2+} is the largest of the three cations, which means that the space between Na^+/Ca^+ on *ab* plane is free in comparison with that between Ba^{2+}. As a result, PO_4 faces can exist on the side of the *ab* plane of Ca^+/Na^+. Therefore, the difference of arrangement of cations along *c*-axis leads to development of new phase $Na_3Ba_2Ca(PO_4)_3$. One Na site in NBC321 was analysed as a split, which could be due to the

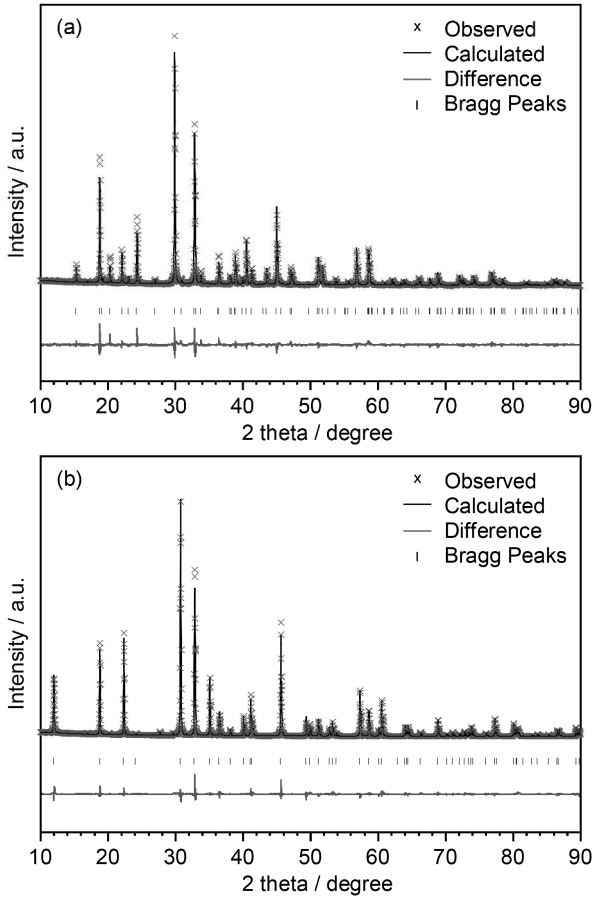

Fig. 3 Rietveld refinement of $NaBa_{1-x}Ca_xPO_4$ powder diffraction for (a) x = 1/3 and (b) x = 0.5 (solid curve: calculated, '×': observed and 'I': Bragg peaks for (a) $Na_3Ba_2Ca(PO_4)_3$ and (b) $NaBa_{0.5}Ca_{0.5}PO_4$.

space, created by oppositely ordered PO_4 units.

Rietveld refinement of the powder diffraction data for x = 1/3 and 0.5 was conducted using the single crystal data as a model structure as shown in Fig. 3. The differences between the calculated and observed patterns are shown at the bottom of each figure. To confirm whether a single phase of NBC321 can be obtained, the sample with x = 1/3 was synthesized. Rietveld refinement using the powder pattern for x = 1/3 revealed that the single phase NBC321 was successfully synthesized. The final reliability factors, R_p, R_{wp} and χ^2 were 6.40 %, 8.58 % and 1.42, respectively. It was also confirmed that NBC321 and its solid solutions were formed with Ca substitution at x = 0.1 - 0.4, and the single phase $Na_3Ba_2Ca(PO_4)_3$ could be obtained at x = 1/3. The single crystal data of NBCP matched the powder diffraction for x = 0.5. Reliability factors, R_p, R_{wp} and χ^2 were 5.21 %, 7.30 %, and 1.46, respectively, indicating that the powder sample for x = 0.5 was a single phase of NBCP without any impurities or secondary phases. Samples with x > 0.5 were also synthesized by 0.1 for x. The samples with x = 1.0 consisted of $NaCaPO_4$ without any other phases. At $0.6 \leq x \leq 0.9$, mixtures of solid solutions of NBCP and $NaCaPO_4$ were formed. No other new phase was obtained at x > 0.5 in the present study.

Photoluminescence properties of Eu^{2+}-activated $NaBaPO_4$, NBC321, and NBCP

Fig. 4 shows the normalized excitation and emission spectra of 1 mol% Eu^{2+}-activated (a) $NaBaPO_4$, NBC321, and (c) NBCP excited at 330 nm. In the absence of Eu, the present samples exhibit practically no emission. Therefore, the observed excitation and emission peaks are attributed to *f-d* transition in Eu^{2+}. $NaBaPO_4$:Eu^{2+} exhibited a maximum emission center at 435 nm, which agrees with a previous report.[15] Ca substitution causes a redshift of the emission center. NBC321:0.01Eu^{2+} and NBCP:0.01Eu^{2+} showed emission maxima at 458 nm and 460 nm, respectively.

Emission lifetime (τ) plots and fitting curves for each sample are shown in Fig. 5. All curves were primarily fitted to a single exponential function. However, to carry out precise fitting, average values calculated using double exponential function were considered in the present study. The results for 1 mol% Eu-doped samples indicated τ = 598 ns for $NaBaPO_4$, 461 ns for NBC321 and 546 ns for NBCP. The value for 1 mol% Eu^{2+}-doped $NaBaPO_4$ is in good agreement with the one (570 ns) reported previously,[15] and the others are in the range of the values reported in Eu^{2+}-doped $ABPO_4$.[16] The τ values for NBC321 and NBCP were smaller than that of the known $NaBaPO_4$ phosphor, however, no clear correlation between τ and the content of Ca in the samples was found.

Eu^{2+} ion is thought to substitute preferentially for Ba^{2+} site considering the ionic radius (Ba^{2+} = 1.61 Å at CN 12) and valence at the Ca^{2+} site. The averages of Ba−O bond lengths in NBC321 and NBCP were found to be 2.938 Å and 2.915 Å, which were shorter than that in $NaBaPO_4$ (3.016 Å). If the relationship between bond lengths remains the same after Eu substitution, a shorter Eu−O bond length would increase the crystal field splitting of the Eu 5*d* orbitals, and as a result, the

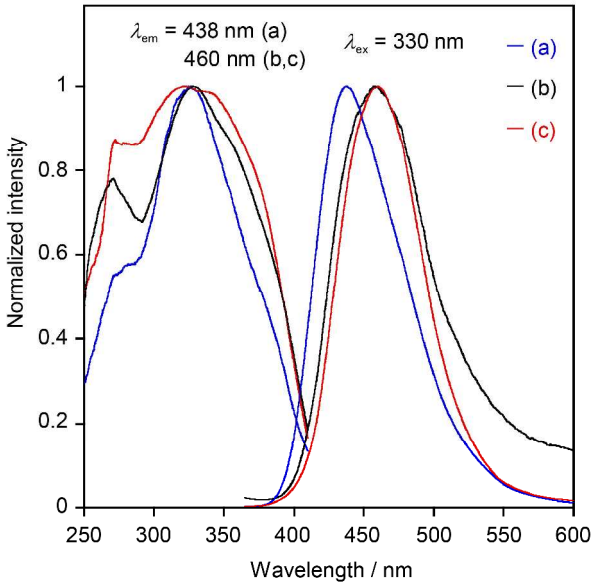

Fig. 4 Normalized excitation and emission spectra of 1 mol% Eu^{2+}-activated (a) $NaBaPO_4$, (b) NBC321, and (c) NBCP.

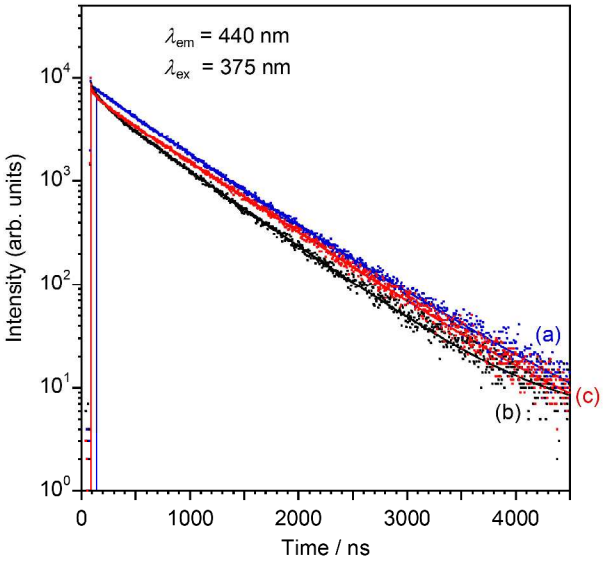

Fig. 5 Emission lifetime (decay) plots and fitting curves for 1 mol% Eu^{2+}-doped (a) $NaBaPO_4$, (b) NBC321 and (c) NBCP (dot: observed, line: fitted).

emission center would be shifted to lower energy with Ca substitution. The internal quantum efficiencies of Eu^{2+}-activated $NaBaPO_4$, NBC321, and NBCP excited at 330 nm were 84 %, 7 %, and 51%, respectively, with the corresponding absorption rates of 76 %, 50 %, and 72 %. One of the reasons for the rather small quantum efficiency in NBC321 system might be concentration quenching in Eu^{2+} ions residing at adjacent Ba sites. It is expected that the photoluminescence properties of new phases can be enhanced by optimization of the synthesis conditions. The excitation spectra covered a range from UV to near UV region, and the phosphors could be excited efficiently under 330 nm. Thus the NBC321 and NBCP may be considered as candidate phosphors for W-LEDs[17] after

the luminescence properties such as emission intensity are improved.

Conclusions

The two new phases, $Na_3Ba_2Ca(PO_4)_3$ and $NaBa_{0.5}Ca_{0.5}PO_4$, were found during the synthesis of $NaBa_{1-x}Ca_xPO_4$ solid solutions by the PC method employing PEG-P. The crystal structures of the new phases were determined to be described as trigonal systems ($P31c$ for NBC321 and $P\text{-}3m1$ for NBCP) by the single crystal XRD analysis. Regularity of PO_4 unit alignment is different among $NaBa_{1-x}Ca_xPO_4$ due to different arrangements of cations. Eu^{2+}-activated samples exhibited blue emission under UV or near UV irradiations. The Ba−O bond length was shortened by Ca ion substitution, and as a result, the wavelength giving the maximum emission in the Eu^{2+}-activated phosphors was red-shifted from 435 nm (for $x = 0$) to 458 nm (for $x = 1/3$) and 460 nm (for $x = 0.5$) under excitation at 330 nm.

Acknowledgements

The authors thank HORIBA for helping us to measure emission lifetime. This work was partially supported by a Grant-in-Aid for Scientific Research (no. 22107002) on Innovative Areas of "Fusion Materials: Creative Development of Materials and Exploration of Their Function through Molecular Control" (no. 2206) from the Ministry of Education, Culture, Sports, Science and Technology, Japan (MEXT) and a Grant-in-Aid for JSPS Fellows (24 - 9285) from Japan Society for the Promotion of Science (JSPS).2

Notes and references

[a]*Institute of Multidisciplinary Research for Advanced Materials, Tohoku University, Sendai 980-8577, Japan*
**E-mail: kakihana@tagen.tohoku.ac.jp*
[b]*Department of Chemistry, Faculty of Science, Okayama University of Science, Okayama 700-0005, Japan*

† Crystallographic Information Frameworks (CIFs) of the $Na_3Ba_2CaPO_4$ and $NaBa_{0.5}Ca_{0.5}PO_4$ obtained from single crystal X-ray analysis. Electronic Supplementary Information (ESI) available: See DOI: 10.1039/b000000x/

1 N. Horosaki, T. Takeda, S. Funahashi and R-J. Xie, *Chem. Mater.,* 2014, **26**, 4280; P. Pust, V. Weiler, C. Hecht, A. Tücks, A. S. Wochnik, A-K. Henß, D. Wiechert, C. Scheu, P. J. Schmidtz and W. Schnick, *Nat. Mater.*, 2014, **13**, 891; P Pust , A. S. Wochnik, E. Baumann, P. J. Schmidt, D. Wiechert, C. Scheu and W. Schnick, *Chem. Mater.*, 2014, **26**, 3544. K. Fujii, Y. Esaki, K. Omoto, M. Yashima, A. Hoshikawa, T. Ishigaki and J. R. Hester, *Chem. Mater.*, 2014, **26**, 2488.

2 L. L. Hench, *J. Am. Ceram. Soc.*, 1991, **74**, 1487.

3 A. K. Padhi, K. S. Nanjundaswamy and J. B. Goodenough, J. Electrochem. Soc., 144, 4, 1188; S. Y. Chung, J. T. Bloking and Y. M. Chiang, *Nature Mater.*, 2002, **1**, 123.

4 S. H. M. Poort, W. Janssen and G. Blasse, *J. Alloys Compd.*, 1997, **260**, 93.

5 T. Hasegawa, H. Kato, Y. Takatsuka, M. Kobayashi, H. Yamane and M. Kakihana, *ECS J. Solid State Sci. Tech.*, 2013, **2**, 3107.

6 J. K. Han, M. E. Hannah, A. Piquette, J. B. Talbot, K. C. Mishra and J. McKittrick, *J. Am. Ceram. Soc.,* 2013, **96**, 1526; S. Choi, Y. J. Yun and H. K. Jung, *Mater. Lett.* 2012, **75**, 186; P. Dai, X. Zhang, L. Bian, S. Lu, Y. Liu and X. Wang, *J. Mater. Chem. C*, 2013, **1**, 4570.

7 M. Kim, M. Kobayashi, H. Kato and M. Kakihana, *Opt. Photonics J.*, 2013, **3**, 13; M. Kim, M. Kobayashi, H. Kato and M. Kakihana, *J. Ceram. Soc. Jpn.*, 2014, **122**, 626.

8 M. Kakihana, *J. Sol-Gel Sci. Technol.*, 1996, **6**, 7; M. Kakihana, M. Yoshimura, *Bull. Chem. Soc. Jpn.*, 1999, **72**, 1427.

9 RAPID-AUTO, Rigaku Corporation, Tokyo, Japan, 2005.

10 T. Higashi, NUMABS – Numerical Absorption Correction, Rigaku Corporation, Tokyo, Japan, 1999.

11 M. C. Burla, R. Caliandro, M. Camalli, B. Carrozzini, G. L. Cascarano, L. De Caro, C. Giacovazzo, G. Polidori, R. Spagna, *J. Appl. Crystallogr.*, 2005, **38**, 381.

12 G. M. Sheldrick, *Acta Crystallogr. Sect. A*, 2008, **64**, 112.

13 L. Farrugia, *J. J. Appl. Crystallogr.*, 1999, **32**, 837.

14 K. Momma and F. Izumi, *J. Appl. Crystallogr.*, 2011, **44**, 1272.

15 S. Zhang, Y. Huang, Y. Nakai, T. Tsuboi and H. J. Seo, *J. Am. Ceram. Soc.*, 2011, **94**, 2987.

16 Y. S. Tang, S. F. Hu, C. C. Lin, N. C. Bagkar and R. S. Liu, *Appl. Phys. Lett.*, 2007, **90**, 151108; C. Qin, Y. Huang, L. Shi, G. Chen, X. Qiao, and H. J. Seo, *J. Phys. D: Appl. Phys.*, 2009, **42**, 185105.; S. Zhang, Y. Nakai, T. Tsuboi., Y. Huang and H. J. Seo, *Inorg. Chem.*, 2011, **50**, 2897.

17 A. Žukauskas, M. S. Shur and R. Gaska, *MRS Bull.*, 2001, **26**, 764; M. H. Chang, D. Das, P. V. Varde, M. Pecht, *Microelectron. Reliab.*, 2012, **52**, 762; V. Bachmann, C. Ronda, A. Meijerink, *Chem. Mater.*, 2009, **126**, 2077; E. F. Schubert and J. K. Kim, *Science* 2005, **308**, 1274.